

## Modeling of wind turbine based on dual DFIG generators

Rabiah Mahroug<sup>1</sup>, Mohamed Matallah<sup>2</sup>, Salam Abudura<sup>3</sup>

<sup>1</sup>Department of Electrical Engineering, Faculty of Technology, University Yahia Fares, Medea, Algeria

<sup>2</sup>Department of Sciences and Technology, Faculty of Science and Technology, University Djilali Bounaama, Khemis Miliana, Algeria

<sup>3</sup>Department of Common Core Technology, University Yahia Fares, Medea, Algeria

### Article Info

#### Article history:

Received Sep 13, 2021

Revised Mar 13, 2022

Accepted Mar 30, 2022

#### Keywords:

DFIG

IFOC

Modeling

Wind turbine

WT-dual-DFIG

### ABSTRACT

In order to investigate a viable approach to fully exploit the wind speed, the present work investigates the application of a novel wind turbine consisting of dual doubly-fed induction generators (DFIG). The model can be further used to apply in areas where the winds are high to achieve high conversion efficiency in order to produce large electric power and increase the wind turbine capacity with an economy of hardware on the one hand, and to reduce the installation cost on the other. Furthermore, this model is always guarantees the continuity of power production because if one generator fails, the second generator will keep working until the broken one is repaired. The proposed model of the wind turbine based on dual doubly-fed induction generators (WT-dual-DFIG) were using the indirect field-oriented control (IFOC) was validated by wind turbine based on single doubly-fed induction generator (WT-single-DFIG) in MATLAB/Simulink. The results of simulation show that the simulated responses of the WT-dual-DFIG increased the power by a factor of about 14.3% compared to a WT-single-DFIG due to the use of a variable speed dual-DFIG. Finally, we can say that the WT-dual-DFIG model is strongly developed and could be applied in the coming years.

*This is an open access article under the [CC BY-SA](https://creativecommons.org/licenses/by-sa/4.0/) license.*



### Corresponding Author:

Rabiah Mahroug

Department of Electrical Engineering, Faculty of Technology, University Yahia Fares

Medea, Algeria

Email: r.mahroug@univ-dbkm.dz

## 1. INTRODUCTION

Due to the lack of conventional energy sources and the increasing formation of pollution emissions in the environment, the researchers and engineers in the design community pay more attention to the advanced technology systems based on sources of renewable energy, like solar and wind energies, and fuel cell [1]. Admittedly, concerns on environmental issues, economic issues, and the rapid growth of population demand for more energy supplies [2], [3]. Undoubtedly, the wind energy source is the most likable choice because of its performance and economic aspects. In addition, conversion systems of wind energy are among the fastest developing technologies and are key to cleanliness and saving power [4], [5].

The technology of wind turbine has developed and became the most promising renewable, clean, and reliable energy source. Since the early 1980s, it has moved very fast from wind energy of a few kilowatts to multi megawatts wind energy [6], [7]. All wind turbine concepts differ in terms of electrical design and control system. Regardless, the technology of wind turbine is a complicated technology that includes many technical disciplines including mechanics, structural dynamics, aerodynamics, meteorology, and electrical engineering that addresses the connection of wind turbines with the power system. As a consequence, it is extremely desired to introduce a novel wind energy system which produces greater power outputs even in areas of low speeds and complex patterns of the wind so as to optimize the effectiveness and the performance

of the aerogenerators and also to benefit of the utmost power that can be generated. With the emergence of wind energy, researchers have devoted their efforts to the development of wind turbine technology, they have done several developments at the level of its components and parts. Consequently, many solutions and control strategies have been investigated in the last decade.

Among the unique researches that were carried out in the last decade, there is the investigation of a diffuser augmented wind turbine (DAWT) studied by researchers [8]-[10]. In these investigations, there was an investigation on a large open-angle controlled diffuser wind energy. Bet and Grassmann [11] suggested a shrouded wind turbine with a wing-profiled ring structure. The result indicated that the use of the DAWT could double the power output of the wing system, as compared with that of the bare wind turbine. A novel system of wind turbine was evolved by Ohya and Karasudani [12], consisting of a diffuser shroud having a broad-ring brim at the exit periphery and inside it a wind turbine. The result showed that the brimmed diffuser shrouded wind turbine has a power increase by a factor of 2 to 5 compared than a bare wind turbine. Among all designs of variable-speed wind turbines, two commercial leading designs are presented on a big scale; synchronous generator SG and wind turbine-based doubly-fed induction generators (DFIG). Without doubt, the DFIG technology has won over other ones; this is due to its cost, reliability, robustness and small requirements of its power converters [3], [13], [14]. DFIG is a three phase asynchronous electric machine with open rotor windings that can be fed by external voltages [15], [16]. DFIG is extensively applied in wind farms power generation because of it has a high in the efficiency and energy quality [17], [18]. Several models of DFIG wind turbine have been suggested recently. A model of order three which is suitable for transient stability analysis was investigated by Lei *et al.* [19]. In addition, Mei and Pal [20] presented a DFIG dynamic model and analyzed the stability of small signal.

In the nonlinear control technologies, an attempt has been suggested to enhance the efficiency and the performance of the DFIG technology. Loucif *et al.* [21] carried out an investigation of a control which is based on sliding mode for the control of real and reactive powers for the rotor and power grid side converters. Besides, Bektache and Boukhezzar *et al.* [22] used a nonlinear predictive controller for a WT-single-DFIG with variable velocity, which improves wind power extraction and reduces temporary loads. The investigators have used nonlinear backstepping control model to realise different purposes of control for wind power systems which are based on DFIG having variable velocity.

The turbine's wind generator is responsible to create electric energy from the mechanical energy. Thus the generator is the most important component in the turbine and can easily fail before reaching the intended life. There are several reasons that can lead the generator to fail. Among these are, weather extremes, wind loading, voltage irregularities, excessive vibration and cooling system failures. Unfortunately, reduced power, inappropriate installation, overspeed, overload, noise, contamination of lubricating substance, vibration, and improper isolation of electricity can lead the generator to break down [23], [24]. The analysis technique of the failure mode and effects analysis (FMECA) is relied upon because it facilitates the identification of potential problems in the design of the processor through by testing the effects of lower-level failures [25]. There are diverse works in the literature that have used FMECA to wind turbine systems. Ozturk *et al.* [24] compared different wind turbine systems and eliminate the underestimation of impacts of different weather conditions by applying the failure modes. Furthermore, Perez *et al.* [26] compared the failure rates and failure values, the results concluded that geared-drive wind turbines have smaller failure rates than direct-drive wind turbines in electrical and electronic components where gearbox failures cause the most failures. Therefore it was necessary to determine the criticality of these different models of wind turbines. The impacts of weather conditions on wind failure systems were examined by Reder *et al.* [27]. The conclusion was that the winter season is the one with high failure frequencies and where wind speed did not give any impact on failure occurrences.

The importance of this research originates with filling the gaps mentioned above by applying the WT-dual-DFIG under the wind speed variation for purposes to extract the maximum of the electrical energy generated and validate the dynamic performances of the wind turbine by simulation using Simulink/MATLAB environment and this proposed model is always guaranteed power production because if one generator fails, the second generator will keep working until the failure is repaired. In order to control the dual generators, a proportional-integrator (PI) controller is used due to its ease of maintenance and simplicity of implementation as compared to other controllers [28], [29].

## 2. NUMERICAL MODELING

### 2.1. Model description

In this work, we propose the model represented in Figure 1, which consists of one turbine, one gearbox and two generators. This typical WT-dual-DFIG where the dual generators were joined to the cycle to produce and extract more electrical energy. We suggested this system in order to produce large electric power and increase the wind turbine capacity with an economy of hardware on the one hand, and to reduce

the installation cost on the other. Furthermore, the advantage of this model is that it always guarantees the continuity of power production because if one generator fails, the second generator will keep working until the broken one is repaired.

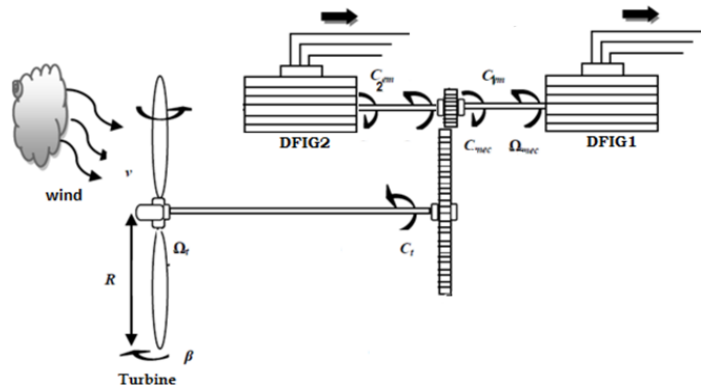


Figure 1. Schematic of conventional dual-DFIG wind model

**2.2. Modelling of the wind**

The wind characteristics give the energy amount which can be extracted from the farm of the wind [30], [31]. The wind speed is defined as a sum of various harmonics [32]:

$$V(t) = 8 + 0.2 * \sin(0.1047.t) + 2 * \sin(0.2665.t) + \sin(1.2930t) + 0.2 * \sin(3.6645t) \quad (1)$$

The model under MATLAB/Simulink illustrated in Figure 2 shows the wind which was given by the modeling of the mathematical formula.

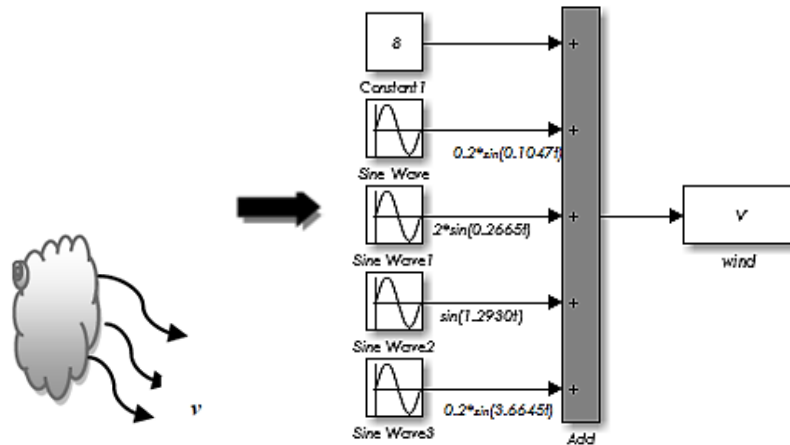


Figure 2. Wind profile model under MATLAB/Simulink

**2.3. Modelling of the turbine**

The technology of wind turbine is utilized to convert part of kinetic into mechanical energy through a wind turbine. The proposed model in the present investigation consists of a wind turbine with a nominal power of 7.9 MW, having a radius= 78m of the blades and driving a dual generator through the gearbox. The production of the wind turbine depends on the interaction between the blade, the wind speed and mass. The performance of the wind turbine quantities such as the power, torque, and speed are determined by the aerodynamic forces generated by the wind. The mechanical and aerodynamic performances of wind turbines are characterised by two main dimensionless parameters: the tip speed ratio  $\lambda$  and the power coefficient  $C_p$  [29]:

$$\lambda = \frac{\Omega_{tur}R}{v} \quad (2)$$

The “power coefficient” presents how efficiently a wind turbine converts the wind power into electrical power. This is given by [30], [33]:

$$C_p(\lambda, \beta) = 0.5176 \left( \left( \left( \frac{116}{\lambda_i} \right) - 0.4\beta - 5 \right) e^{\left( \frac{21}{\lambda_i} \right)} + 0.0068\lambda \right) \quad (3)$$

Where  $\lambda_i$  is given by [19]:

$$\frac{1}{\lambda_i} = \frac{1}{(\lambda + 0.08\beta)} - \frac{0.035}{(\beta^3 + 1)} \quad (4)$$

- $\lambda$  : The tip speed ratio;  
 $\Omega_{tur}$  : The turbine mechanic angular velocity (rad/s);  
 $R$  : The turbine radius (m);  
 $V$  : The wind speed (m/s);  
 $\beta$  : The pitch angle

The kinetic to mechanical energy conversion is performed by the wind turbine which produces torque. The aerodynamic power is given by [32] :

$$P_m = \frac{1}{2} \rho A V^3 \quad (5)$$

Where:  $\rho$  is the air density 1.225kg/m<sup>3</sup> at atmospheric pressure at 15°C and  $A$  is the circular area. Using wind aerodynamic energy, aerodynamic power can be produced by the turbine. It given by [32], [34], [35]:

$$P_v = \frac{1}{2} C_p(\lambda, \beta) \rho \pi R^2 V^3 \quad (6)$$

The aerodynamic torque is given by [30], [36]:

$$C_{aer} = \frac{P_{aer}}{\Omega_{tur}} = \frac{1}{2\Omega_{tur}} C_p(\lambda, \beta) \rho \pi R^2 V^3 \quad (7)$$

#### 2.4. Modelling of the gearbox

The gearbox role is the transformation of the wind turbine speed of speed of the generator, and of the aerodynamic torque to the gearbox torque. It given by the mathematical forms [30]:

$$\Omega_{mec} = G \Omega_{tur} \quad (8)$$

Where

- $G$  : is the multiplication ration;  
 $\Omega_{tur}$  and  $\Omega_{mec}$  : are the mechanical and generator speeds.

The multiplication ration connected the torque on the slow axis and on the fast axis (generator1 and generator2 sides) by:

$$C_{mec} = \frac{C_{aer}}{G} \quad (9)$$

- $C_{mec}$  : Torque applied on the shaft of the generator1 and generator2 (N.m);  
 $C_{aer}$  : Torque applied on the shaft of turbine.

Below is the fundamental equation of dynamics of the shaft model giving the evolution of the mechanical velocity in terms of the total mechanical torque applied to generators 1 and 2 [29], [36]:

$$J_T \frac{d\Omega_{mec}}{dt} = \sum C = C_T - C_{vis} \quad (10)$$

$J_T$  : Total inertia on the shaft, the generator1, the generator2 and containing inertia of the wind turbine:

$$J_T = \frac{J_{tur}}{G^2} + J_{générateur1} + J_{générateur2}$$

The viscous friction torque is:  $C_{vis1} = f_T \Omega_{mec}$

$f_T$  : is the total friction coefficient of the mechanical coupling.

The total torque, which is equal to the superposition of the generator1 and electromagnetic torques, is given by:  $C_T = C_{mec} + C_{em1} + C_{em2}$

$C_{em1}, C_{em2}$  : The electromagnetic torques of the DFIG1 and DFIG2 respectively.

The model under MATLAB/Simulink illustrated in Figure 3 shows the entire chain of the wind turbine, and was given by modelling the mathematical formulas obtained:

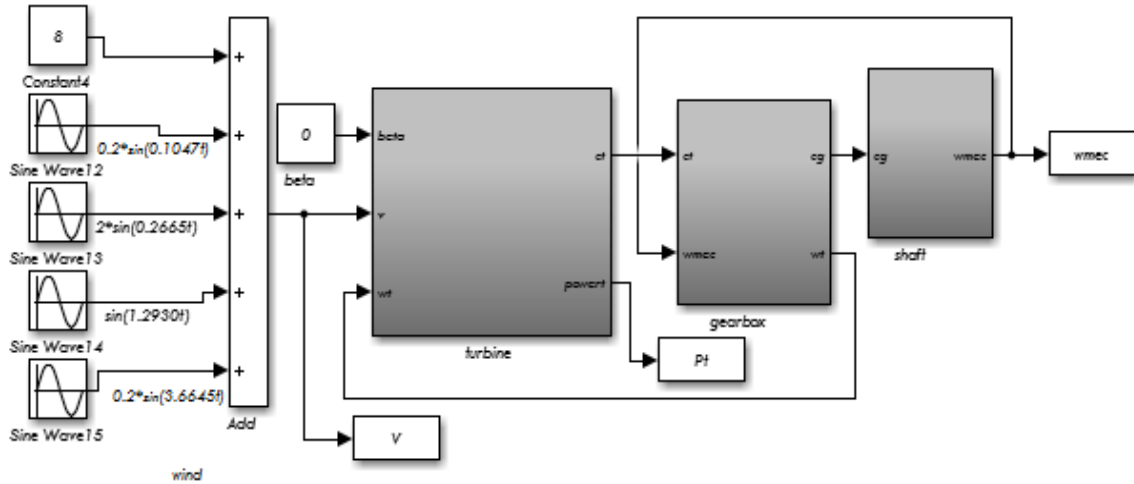


Figure 3. MATLAB/Simulink model for wind turbine

### 2.5. DFIG modeling

Most of the generators used in wind power generation systems are asynchronous generators. They are robust and their cost is relatively low. In this research, we will be interested in the DFIG, most used in wind turbines rotating at a variable speed. The electrical equations of DFIG in the stationary abc reference frame can be given by [32]:

$$\begin{cases} [V_{sabc}] = [R_s] \cdot [I_{sabc}] + \frac{d}{dt} [\varphi_{sabc}] \\ [V_{rabc}] = [R_r] \cdot [I_{rabc}] + \frac{d}{dt} [\varphi_{rabc}] \end{cases} \quad (11)$$

Where:

$$[V_{sabc}] = \begin{bmatrix} V_{sa} \\ V_{sb} \\ V_{sc} \end{bmatrix} \text{ and } [V_{rabc}] = \begin{bmatrix} V_{ra} \\ V_{rb} \\ V_{rc} \end{bmatrix} : \text{The stator\_rotor voltages.}$$

$[I_{sabc}]$  and  $[I_{rabc}]$ : are the stator\_rotor currents;  
 $[\varphi_{sabc}]$  and  $[\varphi_{rabc}]$ : are the stator\_rotor flux linkages;  
 $[R_s]$  and  $[R_r]$  : are stator\_rotor resistance matrices.

The magnetic equations of DFIG are written by [32]:

$$\begin{cases} [\varphi_{sabc}] = [L_{ss}] \cdot [I_{sabc}] + [M_{sr}] \cdot [I_{rabc}] \\ [\varphi_{rabc}] = [L_{rr}] \cdot [I_{rabc}] + [M_{rs}] \cdot [I_{sabc}] \end{cases} \quad (12)$$

By replacing (12) in (11), we obtain the system of (13):

$$\begin{cases} [V_{sabc}] = [R_s] \cdot [I_{sabc}] + \frac{d}{dt} [[L_{ss}] \cdot [I_{sabc}] + [M_{sr}] \cdot [I_{rabc}]] \\ [V_{rabc}] = [R_r] \cdot [I_{rabc}] + \frac{d}{dt} [[L_{rr}] \cdot [I_{rabc}] + [M_{rs}] \cdot [I_{sabc}]] \end{cases} \quad (13)$$

The fundamental equation of the dynamics of DFIG is written by:

$$C_{em} = C_r + f_r \Omega + J \frac{d\Omega}{d\theta} \quad (14)$$

$C_{em}$  and  $C_r$ : The electromagnetic\_resistant torque of the DFIG;

$f_r$ : Friction coefficient of the DFIG;

$\Omega$ : The generator angular rotation velocity (r/min or rad/sec);

$J$ : The total inertia.

The electromagnetic equations of the torque can be given by:

$$C_{em} = p[I_{sabc}]^t \frac{d}{d\theta} [[M_{sr}][I_{rabc}]] \quad (15)$$

$p$ : is the number of DFIG pole pairs.

The three-phase quantities (abc) are transformed to the two-phase rotating quantities (dq) via the Park transformation which reduces the number of equations and simplifies them. We obtain the following electrical equations [33], [37], [38]:

$$\begin{cases} V_{d-s} = R_s I_{d-s} + \frac{d\varphi_{d-s}}{dt} - \omega_s \varphi_{q-s} \\ V_{q-s} = R_s I_{q-s} + \frac{d\varphi_{q-s}}{dt} - \omega_s \varphi_{d-s} \\ V_{d-r} = R_r I_{d-r} + \frac{d\varphi_{d-r}}{dt} - \omega_r \varphi_{q-r} \\ V_{q-r} = R_r I_{q-r} + \frac{d\varphi_{q-r}}{dt} - \omega_r \varphi_{d-r} \end{cases} \quad (16)$$

The magnetic equations in the two-phase reference (dq) are [35], [38], [39]:

$$\begin{cases} \varphi_{d-s} = L_s I_{d-s} + M I_{d-r} \\ \varphi_{q-s} = L_s I_{q-s} + M I_{q-r} \\ \varphi_{d-r} = L_r I_{d-r} + M I_{d-s} \\ \varphi_{q-r} = L_r I_{q-r} + M I_{q-s} \end{cases} \quad (17)$$

Where:  $\omega_r = \omega_s - \omega$ ,  $\omega = p\Omega$

$V_{d-s}, V_{q-s}, V_{d-r}$  and  $V_{q-r}$ : are the direct stator\_rotor voltages in a dq reference;

$I_{d-s}, I_{q-s}, I_{d-r}$  and  $I_{q-r}$ : are the direct stator\_rotor currents in a dq reference;

$\varphi_{d-s}, \varphi_{q-s}, \varphi_{d-r}$  and  $\varphi_{q-r}$ : are the direct stator\_rotor fluxes in a dq reference;

$\omega_s, \omega_r, \omega_s, \omega_r$ : are the stator\_rotor angular speed.

The expression of the electromagnetic torque is represented in (18) [40]:

$$\begin{cases} C_{em} = -P \frac{M}{L_r} (\varphi_{d-r} I_{q-s} - \varphi_{q-r} I_{d-s}) \\ C_{em} = P \frac{M}{L_s} (\varphi_{d-s} I_{q-r} - \varphi_{q-s} I_{d-r}) \end{cases} \quad (18)$$

The active and reactive stator power equations of DFIG under d-q rotating reference are [35]:

$$\begin{cases} P_s = -(I_{d-s} V_{d-s} + I_{q-s} V_{q-s}) \\ Q_s = -(I_{d-s} V_{q-s} - I_{q-s} V_{d-s}) \end{cases} \quad (19)$$

$P_s$  and  $Q_s$ : are the active\_reactive stator powers. With the mathematical equations for computing the active and reactive powers of rotor side [35]:

$$\begin{cases} P_r = (I_{q-r} V_{q-r} + I_{d-r} V_{d-r}) \\ Q_r = -(I_{d-r} V_{q-r} - I_{q-r} V_{d-r}) \end{cases} \quad (20)$$

$P_r$  and  $Q_r$ : The active\_reactive rotor powers.

## 2.6. Field oriented power control

### 2.6.1. Principle of power control

The Park reference dq permits us the creation a natural decoupling of the quantities (d,q) [41]. We are interested in this study to use the vector control method by the stator flux orientation. Two phases dq linked to the rotating reference frame were used on the one hand, and the stator flux is oriented along the d on the other. The equation of the flux was written by [42]:

$$\begin{cases} \varphi_{d-s} = \varphi_s \\ \varphi_{q-s} = 0 \end{cases} \quad (21)$$

In this case the equations of flux are expressed as (22).

$$\begin{cases} 0 = L_s I_{q-s} + M I_{q-r} \\ \varphi_s = L_s I_{d-s} + M I_{d-r} \\ \varphi_{d-r} = \sigma L_r I_{d-r} + \frac{M}{L_s} \varphi_{d-s} = \left( L_r - \frac{M^2}{L_s} \right) I_{d-r} + \frac{M}{L_s} \varphi_s \\ \varphi_{q-r} = \sigma L_r I_{q-r} = \left( L_r - \frac{M^2}{L_s} \right) I_{q-r} \end{cases} \quad (22)$$

The coefficient of the dispersion is:

$$\sigma = 1 - \frac{M^2}{L_s L_r}$$

The Rs is negligible and the regime is permanent, then becomes (23).

$$\begin{cases} V_{d-s} = R_s I_{d-s} + \frac{d\varphi_{d-s}}{dt} \approx 0 \\ V_{q-s} = R_s I_{q-s} + \omega_s \varphi_{d-s} = V_s \approx \omega_s \varphi_s \end{cases} \quad (23)$$

The rotor voltages are expressed as (24).

$$\begin{cases} V_{d-r} = R_r I_{d-r} + \left( L_r - \frac{M^2}{L_s} \right) \frac{dI_{d-r}}{dt} + \left( L_r - \frac{M^2}{L_s} \right) \omega_r I_{q-r} \\ V_{q-r} = R_r I_{q-r} + \left( L_r - \frac{M^2}{L_s} \right) \frac{dI_{q-r}}{dt} - \left( L_r - \frac{M^2}{L_s} \right) \omega_r I_{d-r} + \omega_r \frac{M}{L_s} \varphi_s \end{cases} \quad (24)$$

The equations of active and reactive powers are expressed as (25) [41].

$$\begin{cases} P_s = -V_s \frac{M}{L_s} I_{q-r} \\ Q_s = V_s \frac{\varphi_s}{L_s} - V_s \frac{M}{L_s} I_{d-r} \end{cases} \quad (25)$$

The expression of electromagnetic torque is written by:

$$C_{em} = P(\varphi_{d-s} I_{q-s} - \varphi_{q-s} I_{d-s}) = -P \varphi_{d-s} \frac{M}{L_s} I_{q-r} \quad (26)$$

The DFIG model equations are illustrated in the block diagram of Figure 4 using MATLAB/Simulink. First order transfer functions for voltages are used.

### 2.6.2. Indirect power control of DFIG

This method of control takes the cross-coupling terms and compensates them, through carrying out decoupled control which includes two rotor currents loops. We are interested in this paper to add a PI regulator in each loop (Figure 5), where the references are directly deduced from imposed machine powers [41]. This model used the PI controller composed of two control loops [42]. The diagram block of rotor current control is given in Figure 6.

## 2.7. The combined system model

This paper presents develop two models of the wind turbine, the first one with a single DFIG generator and the second WT-dual-DFIG, followed by a comparison between them. We implement in detail these systems using the MATLAB/Simulink (see Figures 7 and 8). The whole system was simulated and then

the indirect field-oriented control (IFOC) was adopted to control the active and reactive stator powers and the electromagnetic torque.

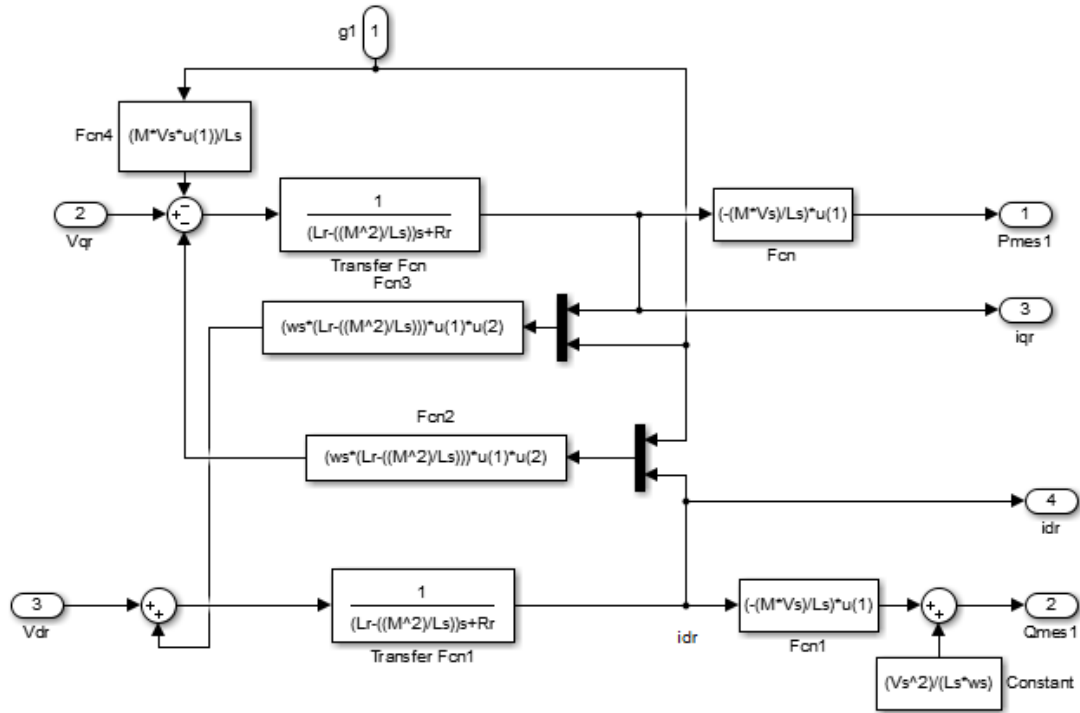


Figure 4. Diagram block of vector control of the DFIG1

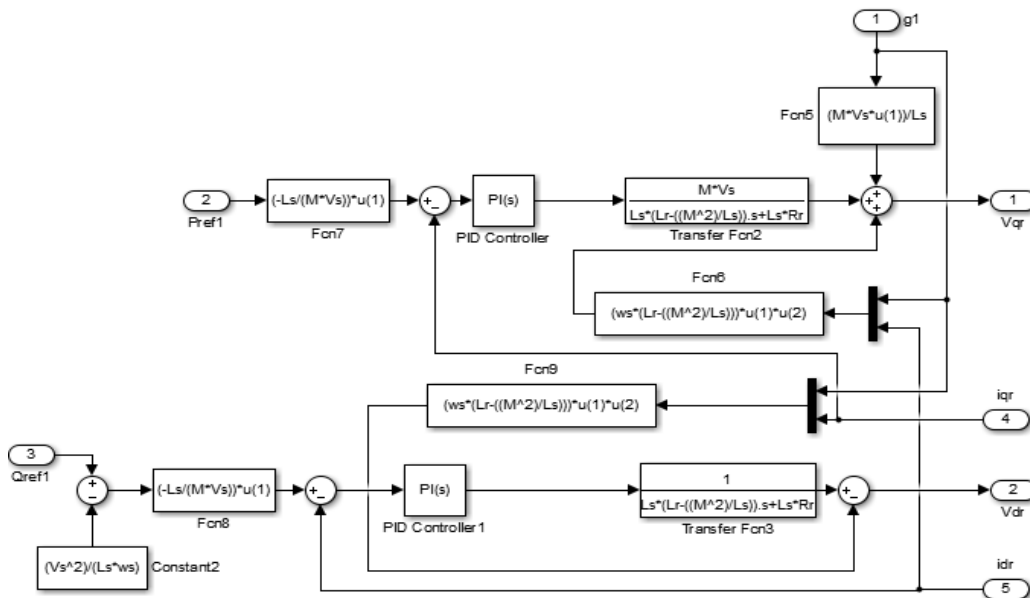


Figure 5. Scheme of indirect power control without power loop using the PI controller

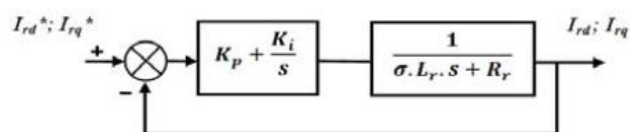


Figure 6. Diagram block of rotor current control



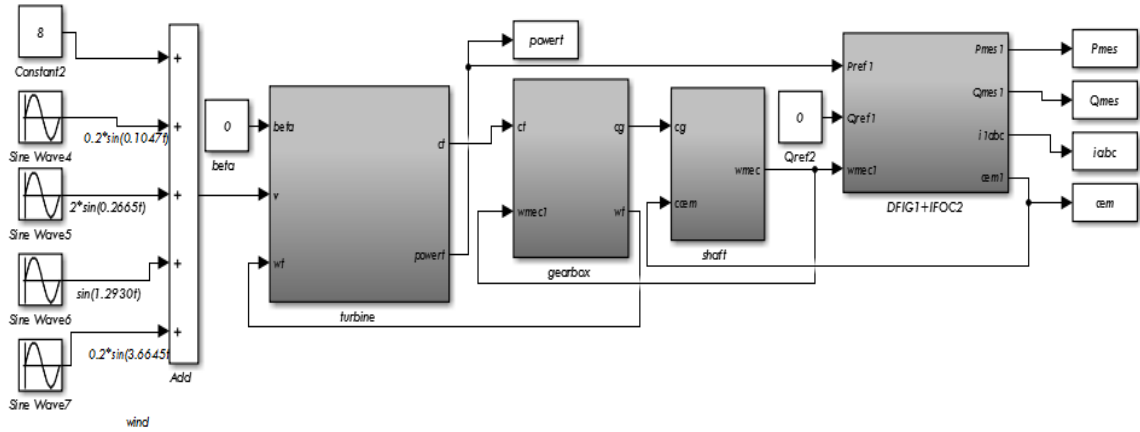


Figure 7. Model of the WT-single-DFIG

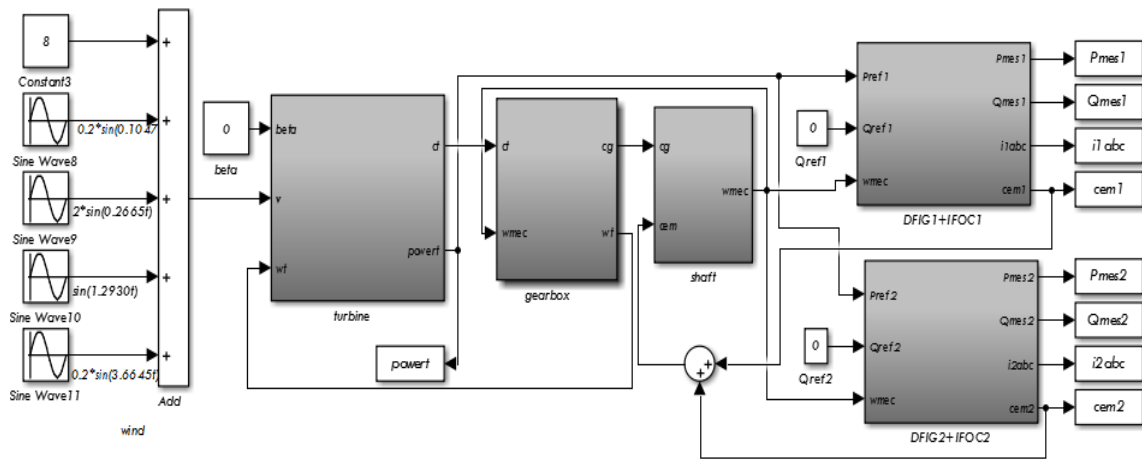


Figure 8. Model of the WT-dual-DFIG

**3. RESULTS AND DISCUSSION**

The MATLAB/Simulink software is utilized to simulation model has been developed to resolve a mathematical model to determine the evolution of various parameters such as active and reactive energy, electromagnetic torque and rotor currents. The reference reactive power is zero. The parameters used in this work are given in Tables 1 and 2.

Table 1. Parameters of DFIG

Parameters	Values
PN	7.9 MW
P	2
M	0.0135 H
Vs	260/690 V
Rr	0.012 Ω
Lr	0.0136 H
J	1000 Kg.m <sup>2</sup>
Rs	0.021 Ω
Ls	0.0137
F	50 Hz
fv	0.0024 Nm/s

Table 2. Parameters of the turbine

Parameters	Values
Diameter	78 m
Gearbox	110
Number of blade	2

**3.1. The results of WT-dual-DFIG**

This part presents an interpretation of the results produced from a wind turbine simulation based on twin DFIG generators, as well as we present a comparison study of our results with other work from the literature based on a different model of wind control [43]. In order to control the electric machines, Bekakra and Attous [43] presented a linear control system based on the sliding mode technique. But this control approach is inconvenient since generator modeling is only done in linear mode, which has no reality, and the results achieved are far from realistic. This research focuses on the IFOC of induction motor to increase the performance of WT-dual-DFIG systems, while keeping in mind that the command is processed with a variation of the machine’s parameters. IFOC motor drives are employed in high-performance systems in a variety of industrial applications because of their comparatively easy set up. The performance simulation results were studied and presented from Figures 9 to 22. As indicated in Figure 9, a random wind profile was applied, ranging from 5 to 11 m/s.

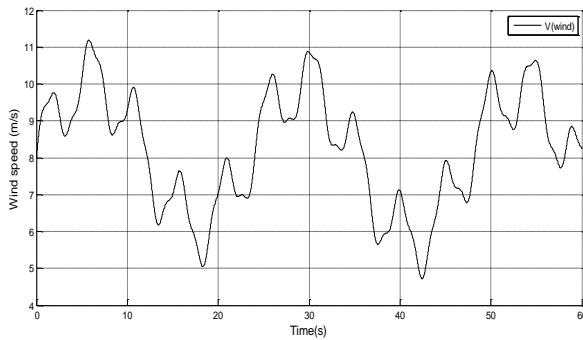


Figure 9. Profile of the wind speed

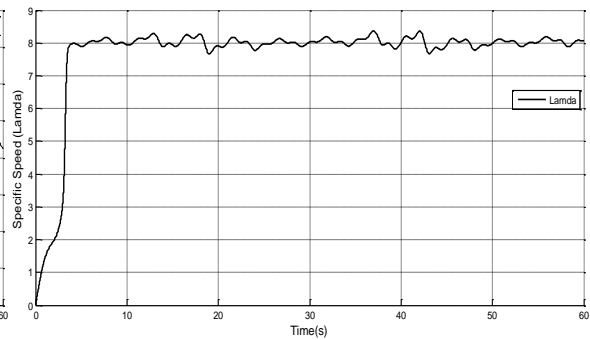


Figure 10. The specific speed

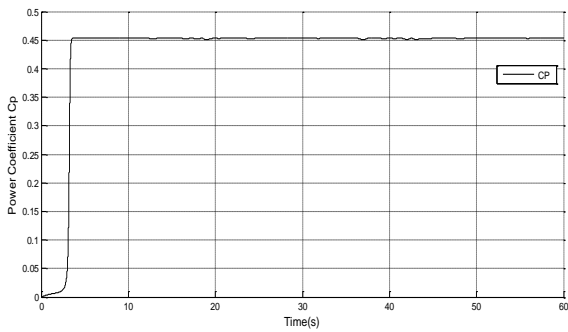


Figure 11. The coefficient Cp

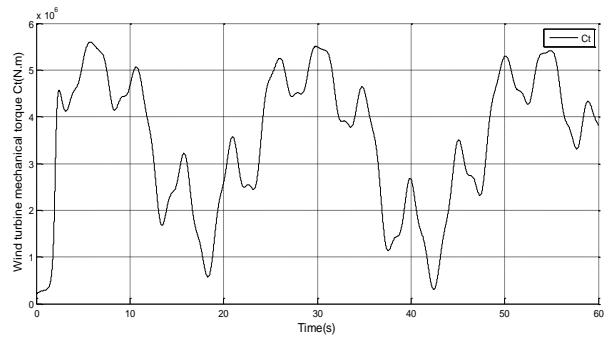


Figure 12. Wind turbine mechanical torque Ct

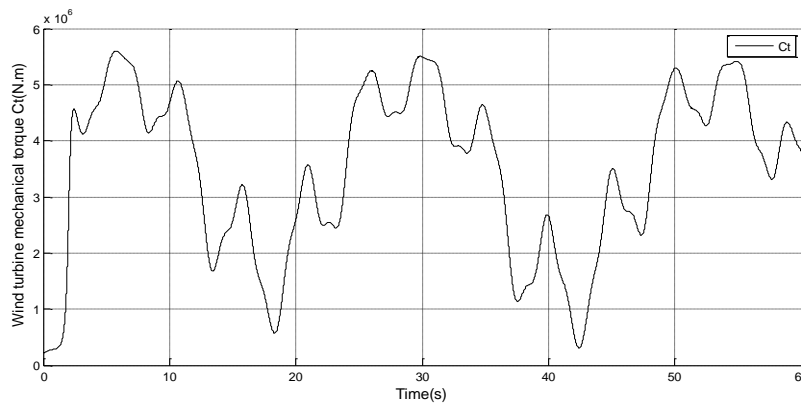


Figure 13. Wind turbine power Pt

For variable wind velocity, Figure 10 presents the evolution of the  $\lambda$  coefficient. The curve always increases during the start-up time and thereafter oscillates around the value ( $\lambda = 8$ ), indicating that the wind profile has an impact on the turbine coefficient. For a variable wind velocity, Figures 11, 12 and 13 show the evolution of the power coefficient  $C_p$ , of the mechanical torque and of the mechanical power of the wind turbine as a function of time respectively. As can be observed, these parameters always increase in the first, then decline and begin to oscillate after that. This clearly demonstrates the impact of the wind profile on the turbine's performance.  $\lambda$  and  $C_p$  vary in response to the wind speed, demonstrating the system's reliability.

Figures 14, 15 and 16 present the electromagnetic torque by the DFIG1, DFIG2 and the proposed model. For the paces of electromagnetic torque, curves reach their maximum values and then they begin to oscillate around their nominal values. The electromagnetic torques of two generators are changed according to the wind turbine is a function of the wind speed.

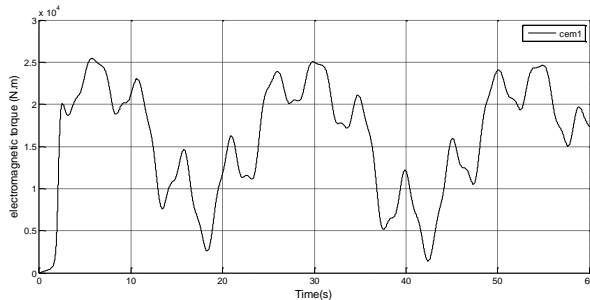


Figure 14. The electromagnetic torque of DFIG1

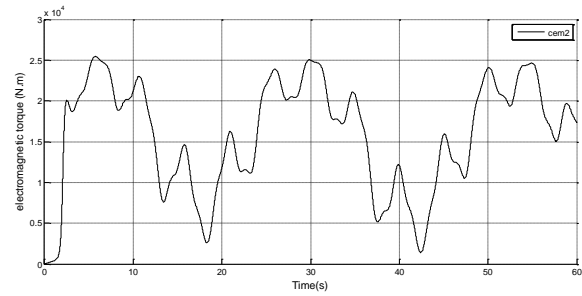


Figure 15. The electromagnetic torque of DFIG2

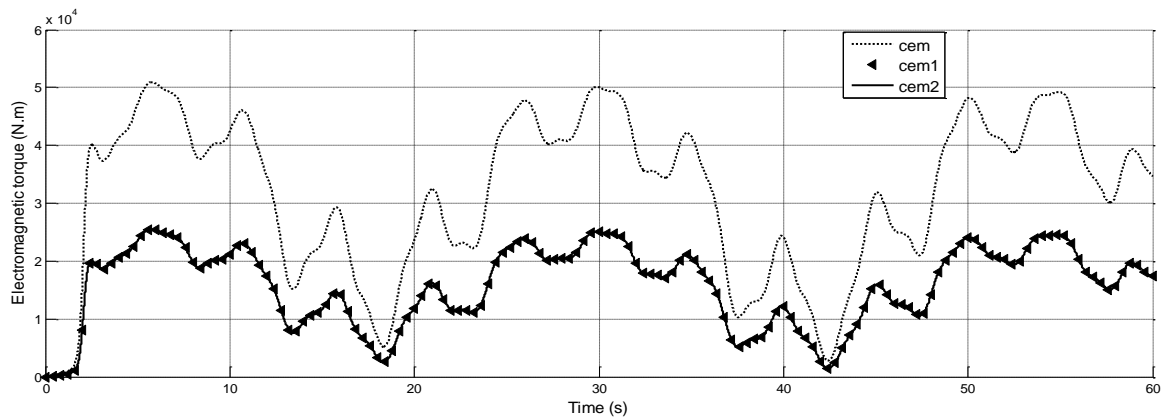


Figure 16. The electromagnetic torque of the proposed model, DFIG1 and DFIG2

Figures 17, 18 and 19 illustrated that the shape of the active power provided by the DFIG1, DFIG2 and the model. It can be seen that the active powers provided by DFIG1 and DFIG2 follow their reference values. The explanation for this is due to the indirect control of the rotor current. For the active power, it decreases and reaches its nominal power. Furthermore, it was noted that the total active power of the proposed model ( $P_{mes}$ ) is two times greater than the active power of each of the two DFIG ( $P_{mes1}$  and  $P_{mes2}$ ). The reference values of the active powers allow us to keep the power coefficient of the wind turbine at its optimum regardless of the wind speed, as shown in Figures 18 and 19. These results are obtained thanks to the IFOC.

Figures 20, 21 and 22 present the reactive power provided by the DFIG1, DFIG2 and the model. It can be regarded that the reactive powers provided by DFIG1 and DFIG2 follow their reference values, and this is due to the indirect control of the rotor current. The reference of the reactive powers (Figures 20, 21 and 22) is fixed at zero so that a unity power factor on the stator side is obtained and the quality of the produced electrical energy is optimised. Both the active and reactive powers follow their references values as desired which increases the robustness of the system.

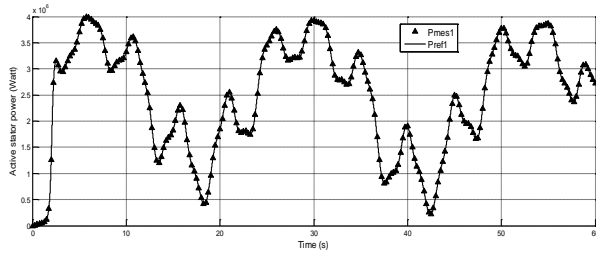


Figure 17. The active stator power of DFIG1

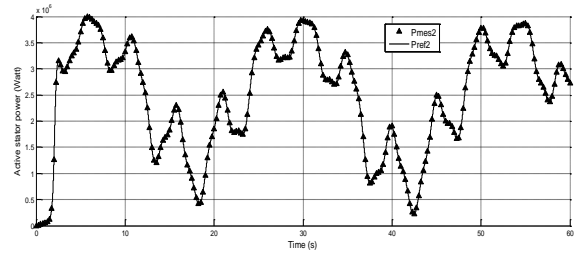


Figure 18. The active stator power of DFIG2

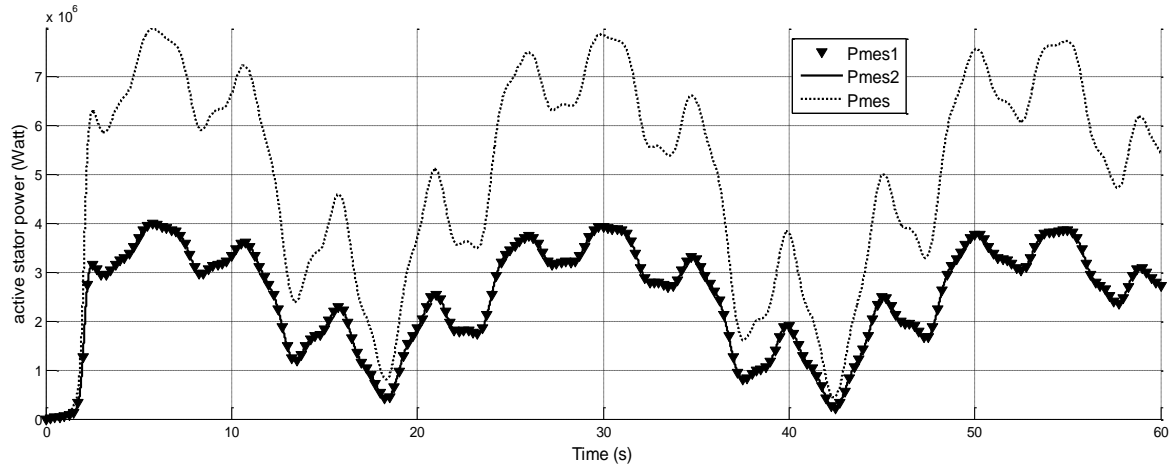


Figure 19. Active stator powers of the proposed model, DFIG1 and DFIG2

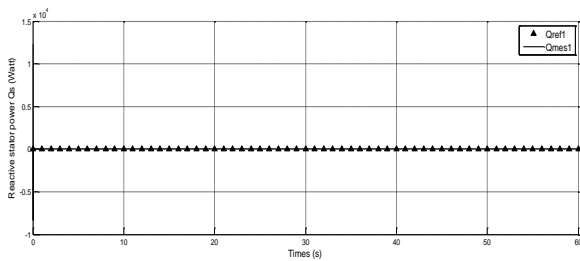


Figure 20. The reactive stator power of DFIG1

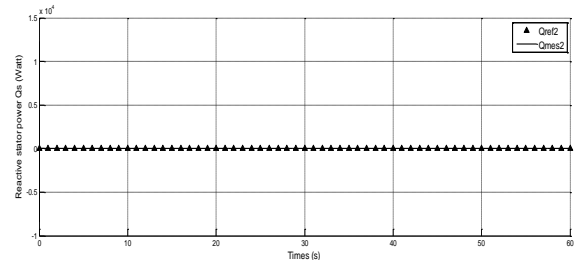


Figure 21. The reactive stator power of DFIG2

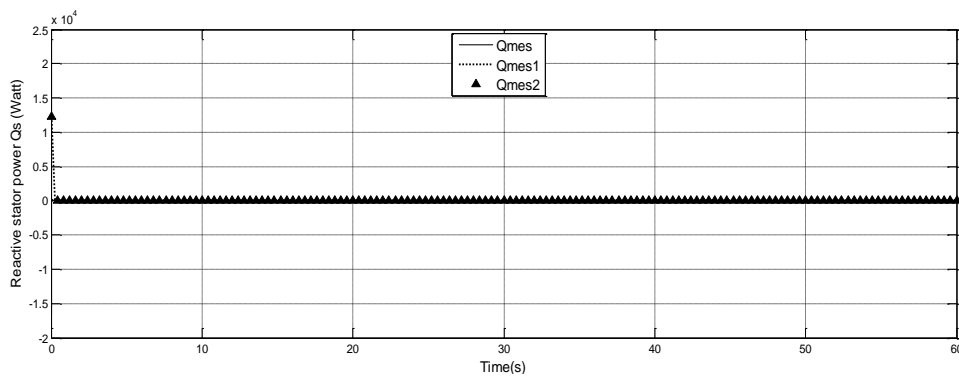


Figure 22. Reactive stator powers of the proposed model, DFIG1 and DFIG2

Figures 23, 24 and 25 show that the three phases of the rotor currents generated by the wind turbine system are sinusoidal with  $f_s=50\text{Hz}$ . It was noted that the total rotor currents of the proposed model are two times greater than the rotor current of each of the two DFIG. This achieved a supply of energy to the grid with good quality. It is believed to behave satisfactorily which confirms the effective performance of IFOC controllers. These figures display the stator currents and we can see that the variations of the magnitudes are as predicted. As presented in the research paper of [43], the speed of the turbine and the power performances are inconsistent and the wind speed reference is not respected. The obtained figures show the different performances of the wind turbine system. They indicate a good robustness, a good reference tracking, and show that the proposed control is reliable and provide better control energy injection into the grid.

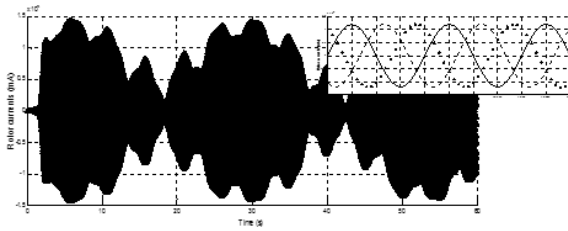


Figure 23. Rotor currents of the DFIG1

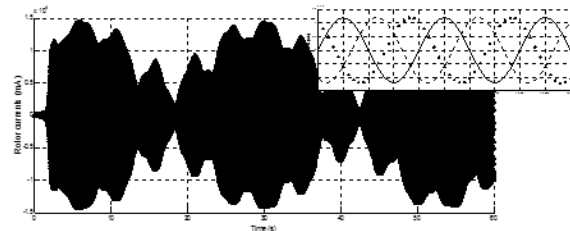


Figure 24. Rotor currents of the DFIG2

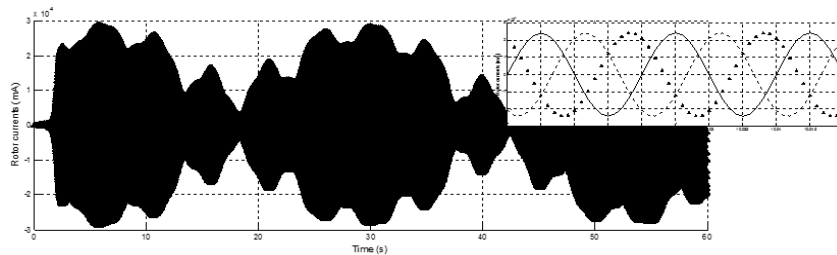


Figure 25. Rotor currents of the proposed model

**3.2. The comparison between the two models**

The validation of the proposed control model was established by performing a simulation of a WT-single-DFIG. The obtained results ensure the robustness and performance of the proposed control model. Figure 26 shows that the wind turbine power of the dual DFIG generators is less than that of the single DFIG generator, and this is due to the electromagnetic torque produced by dual-DFIG generators. But despite this we note in Figure 27 that the active stator power of wind turbine dual DFIG is greater than the active stator power of WT-single DFIG, the difference being more than 1MW. For the time=30s the active stator powers of WT-dual-DFIG=7.86e+6Watt but for WT-single-DFIG=6.85e+6Watt, and from the Figure 27 the comparative between these two models, indicated that the model of the WT-dual-DFIG model offers several advantages such as more productive in power can be reached at 14.3% from the second oscillation than WT-single-DFIG model.

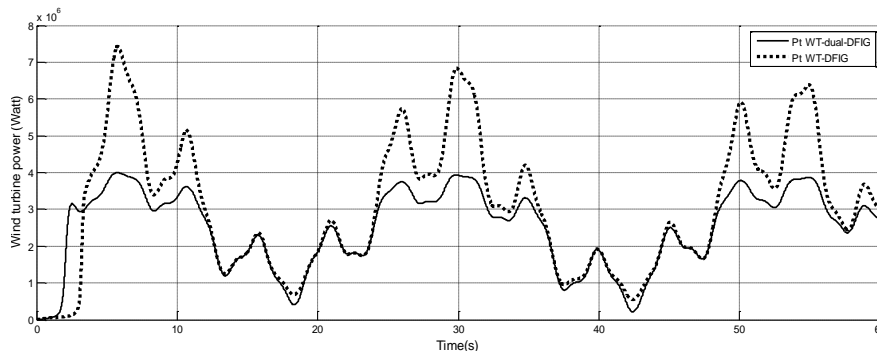


Figure 26. Wind turbine powers of WT-single-DFIG and WT-dual-DFIG

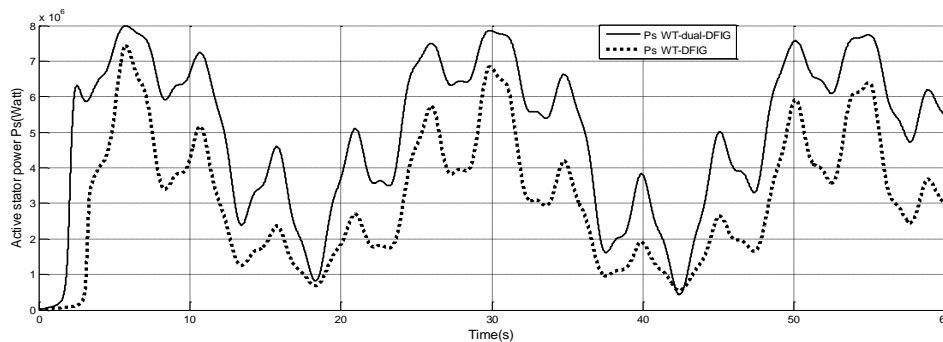


Figure 27. Active stator powers of WT-single-DFIG and WT-dual-DFIG

#### 4. CONCLUSION

This research presented the modeling and simulation of a WT-dual-DFIG operating at a variable speed. The proposed system was implemented in detail using Matlab/Simulink. Whereas, indirect field directed control (IFOC) has been adopted to control the active and reactive stator powers, and the electromagnetic torques. To validate this novel model, a simulation was performed using the WT-single-DFIG model.

The WT-dual-DFIG generators model is more productive in power can be reached at 14.3% compared to WT-single-DFIG generator model especially for large turbine systems. The IFOC offers various advantages like the linearization and the robustness and of the model. The results obtained were satisfactory to ensure the performances of the proposed model. This model guarantees the continuity of power production because if one generator fails, the second generator will keep working until the breakdown is repaired. The maximum energy produced by WT-dual-DFIG model is twice as high as that produced by the WT-single-DFIG generator model.

Results have shown that the dual DFIG model is one of the best alternative solutions in order to generate more energy from economically, energy and environmental protection. In the context of protecting generators and avoiding the low voltage switching problem (LVRT), it is necessary to develop protection systems and artificial intelligence control systems to detect generator failures.

#### ACKNOWLEDGEMENTS




The authors thank University Yahia Fares of Medea and University Djilali Bounaama of Khemis Miliana for their research assistance.

#### REFERENCES




- [1] B. C. Babu and K. B. Mohanty, "Doubly-fed induction generator for variable speed wind energy conversion systems-modeling & simulation," *Int. J. Comput. Electr. Eng.*, vol. 2, no. 1, pp. 141-147, 2010, doi: 10.7763/IJCEE.2010.V2.127.
- [2] M. M. Mansouri, M. Nayeripour, and M. Negnevitsky, "Internal electrical protection of wind turbine with doubly fed induction generator," *Renew. Sustain. Energy Rev.*, vol. 55, pp. 840-855, 2016, doi: 10.1016/j.rser.2015.11.023.
- [3] M. S. Nazir and A. N Abdalla, "The robustness assessment of doubly fed induction generator-wind turbine during short circuit," *Energy Environ.*, vol. 31, no. 4, pp. 570-582, 2020, doi: 10.1177/0958305X19880879.
- [4] K. Noussi, A. Abouloifa, H. Katir, I. Lachkar, and F. Giri, "Nonlinear control of grid-connected wind energy conversion system without mechanical variables measurements," *Int. J. Power Electron. Drive Syst.*, vol. 12, no. 2, pp. 1141-1151, 2021, doi: 10.11591/ijpeds.v12.i2.pp1139-1149.
- [5] B. Wu, Y. Lang, N. Zargari, and S. Kouro, "Power conversion and control of wind energy systems," Hoboken, New Jersey: Wiley-IEEE Press, 2011.
- [6] G. M. J. Herbert, S. Iniyar, E. Sreevalsan, and S. Rajapandian, "A review of wind energy technologies," *Renew. Sustain. Energy Rev.*, vol. 11, no. 6, pp. 1117-1145, 2007, doi: 10.1016/j.rser.2005.08.004.
- [7] Z. Chen and F. Blaabjerg, "Wind energy: the world's fastest growing energy source," *IEEE Power Electron. Soc. Newsl.*, vol. 18, no. 3, pp. 15-19, 2006.
- [8] B. L. Gilbert, R. A. Oman, and K. M. Foreman, "Fluid dynamics of diffuser-augmented wind turbines," *J. Energy*, vol. 2, no. 6, pp. 368-374, 1978, doi: 10.2514/3.47988.
- [9] B. L. Gilbert and K. M. Foreman, "Experiments with a diffuser-augmented model wind turbine," *Energy Resour. Technol. Trans. ASME*, vol.105, no.1, pp. 46-53, 1983, doi: 10.1115/1.3230875.
- [10] O. Igra, "Research and development for shrouded wind turbines," *Energy Convers. Manag.*, vol. 21, no. 1, pp. 13-48, 1981, doi: 10.1016/0196-8904(81)90005-4.
- [11] F. Bet and H. Grassmann, "Upgrading conventional wind turbines," *Renew. Energy*, vol. 28, no. 1, pp. 71-78, 2003, doi: 10.1016/S0960-1481(01)00187-2.
- [12] Y. Ohya and T. Karasudani, "A shrouded wind turbine generating high output power with wind-lens technology," *Energies*, vol. 3, no. 4, pp. 634-649, 2010, doi: 10.3390/en3040634.

- [13] V. Meenakshi and S. Paramasivam, "Control strategy used in DFIG and PMSG based wind turbines an overview," *Int. J. Power Electron. Drive Syst.*, vol. 8, no. 3, pp. 1160-1167, 2017.
- [14] M. A. S. Ali, "Utilizing active rotor-current references for smooth grid connection of a DFIG-based wind-power system," *Adv. Electr. Comput. Eng.*, vol. 20, no. 4, pp. 91-99, 2020, doi: 10.4316/AECE.2020.04011.
- [15] M. Benmeziane, S. Zebirate, A. Chaker, and Z. Boudjema, "Fuzzy sliding mode control of doubly-fed induction generator driven by wind turbine," *Int. J. Power Electron. Drive Syst.*, vol. 10, no. 3, pp. 1592-1602, 2019, doi: 10.11591/ijpeds.v10.i3.pp1592-1602.
- [16] K. Belgacem, A. Mezouar, and N. Essounbouli, "Design and analysis of adaptive sliding mode with exponential reaching law control for double-fed induction generator based wind turbine," *Int. J. Power Electron. Drive Syst.*, vol. 9, no. 4, p. 1534, 2018, doi: 10.11591/ijpeds.v9.i4.pp1534-1544.
- [17] I. El Karaoui, M. Maaroufi, and B. Bossoufi, "Robust power control methods for wind turbines using DFIG-generator," *Int. J. Power Electron. Drive Syst.*, vol. 10, no. 4, p. 2101, 2019, doi: 10.11591/ijpeds.v10.i4.2101-2117.
- [18] B. Bossoufi, M. Karim, S. Ionita, A. Lagrioui, and H. Mahmoudi, "Indirect sliding mode control of a permanent magnet synchronous machine: FPGA-based implementation with MATLAB & simulink simulation," *J. Theor. Appl. Inf. Technol.*, vol. 29, no. 1, pp. 32-42, 2011.
- [19] Y. Lei, A. Mullane, G. Lightbody, and R. Yacamini, "Modeling of the wind turbine with a doubly fed induction generator for grid integration studies," *IEEE Trans. Energy Convers.*, vol. 21, no. 1, pp. 257-264, 2006, doi: 10.1109/TEC.2005.847958.
- [20] F. Mei and B. C. Pal, "Modelling and small-signal analysis of a grid connected doubly-fed induction generator," in *IEEE Power Engineering Society General Meeting*, 2005, pp. 2101-2108, doi: 10.1109/PES.2005.1489386.
- [21] M. Loucif, A. Boumediene, and A. Mechernene, "Nonlinear sliding mode power control of DFIG under wind speed variation and grid connexion," *Electroteh. Electron. Autom.*, vol. 63, no. 3, pp. 23-32, 2015.
- [22] A. Bektache and B. Boukhezzar, "Nonlinear predictive control of a DFIG-based wind turbine for power capture optimization," *Int. J. Electr. Power Energy Syst.*, vol. 101, pp. 92-102, 2018, doi: 10.1016/j.ijepes.2018.03.012.
- [23] S.-H. G. Teng and S.-Y. M. Ho, "Failure mode and effects analysis: an integrated approach for product design and process control," *Int. J. Qual. Reliab. Manag.*, vol. 13, no. 5, pp. 8-26, 1996, doi: 10.1108/02656719610118151.
- [24] S. Ozturk, V. Fthenakis, and S. Faulstich, "Failure modes, effects and criticality analysis for wind turbines considering climatic regions and comparing geared and direct drive wind turbines," *Energies*, vol. 11, no. 9, p. 2317, 2018, doi: 10.3390/en11092317.
- [25] H. Pentti and H. Atte, "Failure mode and effects analysis of software-based automation systems," *VTT Ind. Syst. STUK-YTO-TR*, vol. 190, p. 190, 2002.
- [26] J. M. P. Pérez, F. P. G. Márquez, A. Tobias, and M. Papaalias, "Wind turbine reliability analysis," *Renew. Sustain. Energy Rev.*, vol. 23, pp. 463-472, 2013, doi: 10.1016/j.rser.2013.03.018.
- [27] M. Reder, N. Y. Yürüşen, and J. J. Melero, "Data-driven learning framework for associating weather conditions and wind turbine failures," *Reliab. Eng. Syst. Saf.*, vol. 169, pp. 554-569, 2018, doi: 10.1016/j.res.2017.10.004.
- [28] M. El Azaoui, H. Mahmoudi, and K. Boudaraia, "Backstepping control of wind and photovoltaic hybrid Renewable Energy System," *Int. J. Power Electron. Drive Syst.*, vol. 7, no. 3, p. 677, Sep. 2016, doi: 10.11591/ijpeds.v7.i3.pp677-687.
- [29] S. Mensou, A. Essadki, T. Nasser, and B. B. Idrissi, "An efficient nonlinear backstepping controller approach of a wind energy conversion system based on a DFIG," *Int. J. Renew. Energy Res.*, vol. 7, no. 4, pp. 1520-1528, 2017.
- [30] B. Benyachou, B. Bahra, and M. Tamani, "Modelling with MATLAB/Simulink of a wind turbine connected to a generator asynchronous dual power (GADP)," *J. Mater. Environ. Sci.*, vol. 8, no. 5, pp. 4614-4621, 2017.
- [31] F. Amrane and A. Chaiba, "A hybrid intelligent control based on DPC for grid-connected DFIG with a fixed switching frequency using MPPT strategy," in *2015 4th International Conference on Electrical Engineering (ICEE)*, 2015, pp. 1-4, doi: 10.1109/INTEE.2015.7416678.
- [32] I. Yaichi, A. Semmah, and P. Wira, "Direct power control of a wind turbine based on doubly fed induction generator," *Eur. J. Electr. Eng.*, vol. 21, no. 5, pp. 457-464, 2019, doi:10.18280/ejee.210508.
- [33] M. Taleb and M. Cherkaoui, "Active and reactive power control of doubly fed induction generator wind turbines to answer grid codes requirements," *J. Clean Energy Technol.*, vol. 6, no. 2, pp. 101-105, 2018, doi: 10.18178/jocet.2018.6.2.442.
- [34] M. Bouderbala, B. Bossoufi, A. Lagrioui, M. Taoussi, H. A. Aroussi, and Y. Ihedrane, "Direct and indirect vector control of a doubly fed induction generator based in a wind energy conversion system," *Int. J. Electr. Comput. Eng.*, vol. 9, no. 3, p. 1531, Jun. 2019, doi: 10.11591/ijece.v9i3.pp1531-1540.
- [35] L. Wang, "Advanced control of variable speed wind turbine based on doubly-fed induction generator," Ph.D. dissertation, Dept. Elect. Eng. Electro., Liverpool Univ., London Campus, England, 2012.
- [36] F. Senani, A. Rahab, and H. Benalla, "A complete modeling and control for wind turbine based of a doubly fed induction generator using direct power control," *Int. J. Power Electron. Drive Syst.*, vol. 8, no. 4, p. 1954, 2017, doi: 10.11591/ijpeds.v8.i4.pp1954-1962.
- [37] O. Zamzoum, Y. El Mourabit, M. Errouha, A. Derouich, and A. El Ghzizal, "Power control of variable speed wind turbine based on doubly fed induction generator using indirect field-oriented control with fuzzy logic controllers for performance optimization," *Energy Sci. Eng.*, vol. 6, no. 5, pp. 408-423, 2018, doi: 10.1002/ese3.215.
- [38] A. Tarfaya, D. Dib, S. Ghoudelbourk, and M. Ouada, "Comparative study of two PWM control wind system based on DFIG and multilevel NPC inverter Etude comparative de deux systèmes éoliens de contrôle MLI basés sur GADA et un onduleur NPC à Multi niveaux," *Rev Sci Technol Synthèse*, vol. 25, no. 1, pp. 97-108, 2019.
- [39] N. El Ouanjli, M. Taoussi, A. Derouich, A. Chebabhi, A. El Ghzizal, and B. Bossoufi, "High performance direct torque control of doubly fed induction motor using fuzzy logic," *Gazi Univ. J. Sci.*, vol. 31, no. 2, pp. 532-542, 2018.
- [40] A. Tarfaya, D. Dib, and M. Ouada, "Study contribution to control optimization of a wind turbine based on a DFIG," *Int. Conf. on Mechanical And Industrial Engineering (ICMAIE'2015)*, June 10-11, 2015, doi: 10.15242/IAE.IAE0615202.
- [41] K. D. E. Kerrouche, A. Mezouar, and L. Boumediene, "The suitable power control of wind energy conversion system based doubly fed induction generator," *Int. J. Comput. Appl.*, vol. 87, no. 3, pp. 35-44, 2014, doi: 10.5120/15191-3570.
- [42] S. Mensou, A. Essadki, I. Minka, T. Nasser, B. B. Idrissi, and L. Bentarla, "Performance of a vector control for DFIG driven by wind turbine: real time simulation using DS1104 controller board," *Int. J. Power Electron. Drive Syst.*, vol. 10, no. 2, pp. 1003-1013, 2019, doi: 10.11591/ijpeds.v10.i2.1003-1013.
- [43] Y. Bekakra and D. B. Attous, "Sliding mode controls of active and reactive power of a DFIG with MPPT for variable speed wind energy conversion," *Aust. J. Basic Appl. Sci.*, vol. 5, no. 12, pp. 2274-2286, 2011.




**BIOGRAPHIES OF AUTHORS**

**Rabiaa Mahroug**    has a degree in machine control engineering from the University of Blida, Algeria (2004), a Magister in nanotechnology from the Universidad Chlef, Algeria (2009). She is currently an assistant professor at the University of Khemis-Miliana, Algeria. Her research interests include renewable energy and wind energy. She can be contacted at email: [m.mahroug@univ-dbkm.dz](mailto:m.mahroug@univ-dbkm.dz).



**Mohamed Matallah**    received his PhD in electrical engineering in 1991 at the University of Swansea, UK. He is currently working as a Professor at the University of Khemis-Miliana, Algeria, and is a member of The LESI (Energies and Intelligent Systems) Laboratory. His research interests include High voltage engineering, power systems, and renewable energies. He can be contacted at email: [m.matallah@univ-dbkm.dz](mailto:m.matallah@univ-dbkm.dz).



**Salam Abudura**    full Professor at the University of Médéa- Algeria. He obtained the title of State Engineer in electro-mechanics in 1991 and Master of science in electro-mechanic engineering in 1993 from Maritime Academy State of Odessa-Ukraine. He has a PhD in energy installations of ships (mechanical engineering) option: automatism-1999. He is President of the Scientific Board of the Faculty of Technology, University of Médéa since 2011 to date. His research interests include asynchronous generator wind-driven complexes, power systems, and renewable energies. He can be contacted at email: [abudura.salam@gmail.com](mailto:abudura.salam@gmail.com).